Thermogravimetric Study of the Ln_2O_3–Co–Co_2O_3 System. VI: Ln = Pr at 1100 and 1150°C

Kenzo Kitayama

Department of Applied Chemistry and Biotechnology, Faculty of Engineering, Niigata Institute of Technology, Fujihashi, Kashiwazaki, Niigata 945-1195, Japan

Phase equilibria in the system Pr–Co–O at 1100 and 1150°C are established by changing the oxygen partial pressure from 0 to 12.00 in $-\log(P_{O_2}/atm)$, and a representative phase diagram at 1100°C is presented for the Pr_2O_3–Co–CO_2O_3 system. Under experimental conditions, the $PrO_{1.63+\alpha}(\sigma)$, Pr_2O_3, CoO, Co, Pr_2CoO_4, $Pr_4Co_3O_{10}$, and $PrCoO_3$ phases are present at both temperatures. The stoichiometric Pr_2CoO_4 is not stable. The nonstoichiometry of the compounds, Pr_2CoO_4, $Pr_4Co_3O_{10}$, and $PrCoO_3$ is represented with respect to the oxygen partial pressure, and activities of the components in the solid solutions are calculated using the composition–oxygen partial pressure relations obtained. The standard Gibbs energy changes of the reactions in the phase diagrams are calculated and their linearity with temperature is confirmed under the present experimental conditions. © 2000 Academic Press

The phase equilibrium in the Pr–Co–O system has been established at 1200°C by author (1). It was clarified in the report that phases Pr_2O_3, Co, CoO, Pr_2CoO_4, $Pr_4Co_3O_{10}$, and $PrCoO_3$ are stable. Moreover, standard Gibbs energy changes of reactions were determined based on the phase diagram obtained, and lattice constants of Pr_2CoO_4, $Pr_4Co_3O_{10}$, and $PrCoO_3$ were determined using quenching samples. The structures and lattice parameters of these compounds, of course, were reported previously (2–5). The pattern of the system is different from that of the La–Co–O system (6), which has the same La_2CoO_4, $La_4Co_3O_{10}$, and $LaCoO_3$ type compounds.

The objectives of the present study are also (1) to establish detailed phase equilibria in the system at 1100 and 1150°C as a function of a oxygen partial pressure, (2) to determine the thermochemical properties based on the phase equilibria at different temperatures, and (3) to ascertain whether the isothermal pattern of the phase diagram of the Pr–Co–O system at 1100 and 1150°C changes for La–Co–O type at 1200°C, in which stoichiometric Pr_2CoO_4 is stable, with temperature or not.

EXPERIMENTALS

Analytical grade Pr_6O_{11} (99.9%) and CoO (99.9%) were used as starting materials. CoO was dried by heating at 1100°C in air. The green Pr_2O_3 was prepared by reducing Pr_6O_{11} in an atmosphere of H_2 and CO_2 at mixture ratio of 1 at 1200°C (7). Mixtures with desired ratios of Pr_2O_3/CoO were prepared by mixing thoroughly in an agate mortar and then were calcined several times during the intermediate mixing and treated using the same procedures as described previously (8).

Mixed gases of CO_2 and H_2 and of CO_2 and O_2 were used to obtain the oxygen partial pressures in the present experiment.

The apparatus and procedures for controlling the oxygen partial pressures and for keeping a constant temperature, the method of thermogravimetry, and the criterion for the establishment of equilibrium were the same as those described in the previous paper (8). The method of establishment of equilibrium is briefly written as follows: to ensure equilibrium, the equilibrated point of each sample at an oxygen partial pressure was established from both sides of reaction, that is to say, from low oxygen partial pressures to high oxygen partial pressures and vice versa. The balance, furnace, and gas mixer are schematically shown (8). The furnace is used vertically, which has a mullite tube wound with Pt 60%–Rh 40% alloy wire as the heating element. Mixed gases, which make desired oxygen partial pressures, pass from the bottom of the furnace to the top.

The identification of phases was performed using a Rigaku X-ray diffractometer Rint 2500-type apparatus, employing Ni-filtered Cu$K\alpha$ radiation.

RESULTS AND DISCUSSIONS

1. Pr–O System at 1100 and 1150°C

The Pr–O system was widely investigated by Hyde *et al.* (9). They reported two wide-range solid solutions at high temperatures: σ, a body-centered cubic phase of a composition ca. $PrO_{1.60}$ to $PrO_{1.70}$, and α, a face-centered cubic

phase of composition ca. $PrO_{1.72}$ to PrO_2. But their results did not show the relationship between the oxygen partial pressure and the composition (of nonstoichiometry). Besides, their data at high temperatures, for example Fig. 2 in (9), were not always reliable, because Fig. 1 in (10) appears to be different from the previous figure (Fig. 2 in (9)). In any way, there yet are discrepancies in the Pr–O system even in the same author's paper. Ramdas *et al.* found phase transitions in the composition region $PrO_{1.50}$–$PrO_{1.71}$ at high temperatures (11), and isobaric gravimetric studies of PrO_x have shown the existence of some nonstoichiometric phases between $PrO_{1.5}$ and $PrO_{2.0}$ (12). Sugihara reported $PrO_{1.5}$ and $PrO_{1.6+x}$ (σ-phase) to be stable phases at 1100° and 1200°C, and the solid solution ranges of $PrO_{1.6+x}$ become wider at 1200°C than at 1100°C (12). The dependency of the composition of the Pr–O system upon the oxygen partial pressure was not apparent.

Consequently, the Pr–O system was reinvestigated at 1100° and 1150°C in the oxygen partial pressure range from $\log(P_{O_2}/\text{atm}) = 0$ to -12.00.

The experimental results at 1100°C were, as an example, illustrated with a relation between $\log(P_{O_2}/\text{atm})$ and the O/Pr mol ratio in Fig. 1. In the experimental conditions, Pr_2O_3 is stable from -12.00 to -1.30. At $\log P_{O_2} = -1.30$ Pr_2O_3 changes to $PrO_{1.63}$, which might be the end composition of the $PrO_{1.63-1.70}$ (σ) solid solution. The solid solution is stable in the oxygen partial pressure from -1.30 to 0 in the present experimental conditions.
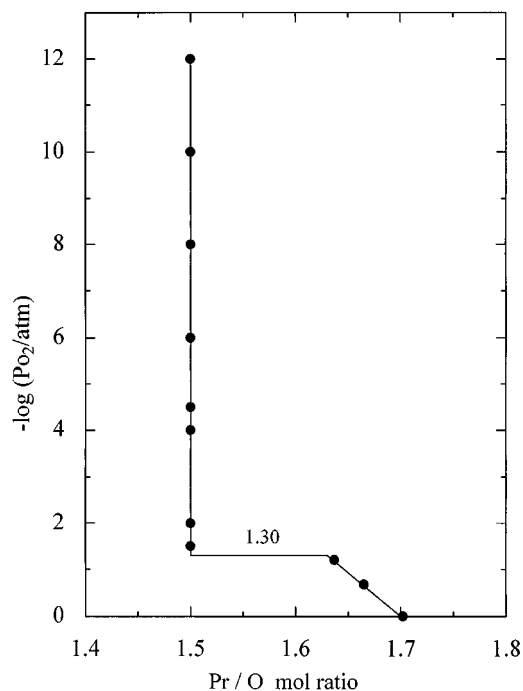

FIG. 1. The relationship between the oxygen partial pressure, $\log(P_{O_2}/\text{atm})$, and O/Pr mole ratio at 1100°C.

Linear relations between the oxygen partial pressure and the composition of the solid solution, $N_O/N_{Pr} = 0.0538 \log P_{O_2} + 1.70$ at 1100°C and $N_O/N_{Pr} = 0.0471 \log P_{O_2} + 1.68$ at 1150°C, are obtained. Here, N_O and N_{Pr} are the mole fraction of oxygen and praseodymium in the solid solution, respectively. From the above equations, O/Pr mol ratios at 1100 and 1150°C are 1.70 and 1.68 at $\log P_{O_2} = 0$, respectively. This means that the compositions of praseodymium oxide at 1100 and 1150°C in 1 atm O_2 are almost equal. These values correspond to Pr_4O_7($PrO_{1.75}$) or Pr_3O_5($PrO_{1.67}$) in 1 atm O_2 rather than Pr_6O_{11}($PrO_{1.83}$), and these are σ phase. But the quenched samples in air and O_2 atmosphere are identified to be Pr_6O_{11} by means of X-ray diffractometry.

At 1150°C Pr_2O_3 is stable in the oxygen partial pressure from -0.94 ± 0.24 to -12.00 in $\log P_{O_2}$. In this report, no further reference to the stable phase of the Pr–O system is made.

2. Pr_2O_3–Co–Co_2O_3 System at 1100°C

The Co–O system was reinvestigated at 1100 and 1150°C using the present apparatus and procedures (8). As shown in Table 1 in the Ref. (8), the oxygen partial pressures in equilibrium with CoO and Co metal at 1100 and 1150°C were 10.33 ± 0.03 and 9.70 ± 0.03 in $-\log(P_{O_2}/\text{atm})$, respectively. Also, x in CoO_x was ~1.000 and 1.012 at 10.33 and 0 in $-\log P_{O_2}$ at 1100°C and 1.000 and 1.011 at 9.70 and 0 in $-\log P_{O_2}$ at 1150°C.

Eight samples with Pr_2O_3/CoO mole ratios of 6/4, 5/5, 0.475/0.525, 4/6, 0.375/0.625, 1/2, 3/7, and 2/8 were prepared for use in thermogravimetry. Break points are found in equilibrium with three solid phase regions at 10.33, 5.86, 4.24, 3.95, 3.50, 2.75, and 1.30 in $-\log P_{O_2}$. The value 10.33 corresponds to the oxygen partial pressure of the reaction, $Co + 1/2 O_2 = CoO$ described above.

Based on the above results of thermogravimetry and of the identifications of phases, a phase diagram is shown in Fig. 2 as Pr_2O_3–Co–Co_2O_3, although Co_2O_3 is not stable under the experimental conditions. The numerical values in the three solid phases in Fig. 2 are the seven values in $-\log P_{O_2}$ described above. Seven phases, Co, CoO, $PrO_{1.63-1.70}$(σ), Pr_2O_3, Pr_2CoO_4, $Pr_4Co_3O_{10}$, and $PrCoO_3$, are stable in the experimental conditions. Co_3O_4 is not found, and the stoichiometric Pr_2CoO_4 is not stable in Fig. 2 in contrast to the La–Co–O system at 1200°C.

The data of compositions of the ternary compounds, symbols, stability ranges in $\log P_{O_2}$, and activities of the components in the solid solutions are shown in Table 1.

Except for Pr_2O_3, the other phases have nonstoichiometric compositions. The relationship between the composition of solid solutions and the oxygen partial pressures is represented by an equation such as a function of the oxygen partial pressure, $N_O/N_{\text{component}} = a \log P_{O_2} + b$, which can

TABLE 1
Composition, Symbols, Stability Ranges in Oxygen Partial Pressure, and Activities of Components in Solid Solutions

Component	Composition	Symbol	$-\log P_{O_2}$ (atm)	$\log a_i$
1100°C				
Pr_2CoO_4	$Pr_2CoO_{4.15}$	A_1	5.86	0
	$Pr_2CoO_{4.16}$	A_2	4.24	−0.122
	$Pr_2CoO_{4.16}$	A_3	3.95	−0.145
$Pr_4Co_3O_{10}$	$Pr_4Co_3O_{9.92}$	B_1	4.24	0
	$Pr_4Co_3O_{9.94}$	B_2	3.95	0.0104
	$Pr_4Co_3O_{9.96}$	B_3	3.50	0.0222
	$Pr_4Co_3O_{10.0}$	B_4	2.75	0.0303
$PrCoO_3$	$PrCoO_{2.90}$	C_1	3.50	0
	$PrCoO_{2.93}$	C_2	2.75	0.0333
	$PrCoO_{3.00}$	C_3	1.30	0.0625
CoO	$CoO_{1.00}$	D_1	10.33	0
	$CoO_{1.00}$	D_2	5.86	~0
	$CoO_{1.00}$	D_3	4.24	~0
	$CoO_{1.01}$	D_4	3.50	~0
1150°C				
Pr_2CoO_4	$Pr_2CoO_{4.09}$	A'_1	5.77	0
	$Pr_2CoO_{4.14}$	A'_2	4.00	−0.104
	$Pr_2CoO_{4.15}$	A'_3	3.65	−0.123
$Pr_4Co_3O_{10}$	$Pr_4Co_3O_{9.97}$	B'_1	4.00	0
	$Pr_4Co_3O_{9.98}$	B'_2	3.65	4.17×10^{-3}
	$Pr_4Co_3O_{9.99}$	B'_3	3.27	7.18×10^{-3}
	$Pr_4Co_3O_{10.0}$	B'_4	2.20	7.27×10^{-3}
$PrCoO_3$	$PrCoO_{2.91}$	C'_1	3.27	0
	$PrCoO_{2.95}$	C'_2	2.20	0.0397
	$PrCoO_{3.00}$	C'_3	0.94	0.0598
CoO	$CoO_{1.00}$	D'_1	9.70	0
	$CoO_{1.00}$	D'_2	5.77	~0
	$CoO_{1.00}$	D'_3	4.00	~0
	$CoO_{1.01}$	D'_4	3.27	~0

FIG. 2. Phase equilibrium in the Pr_2O_3–Co–Co_2O_3 system at 1100°C. Numerical values in the three phase regions are the oxygen partial pressures in $-\log(P_{O_2}/\text{atm})$ in equilibrium with three solid phases. Abbreviations are the same as those in Table 1.

In Table 2, phases present under invariant conditions at 1100° and 1150°C are presented although some results are apparent from Fig. 2 and Table 1.

4. The Standard Gibbs Energy Changes of Reaction and Its Dependency on Temperature

On the basis of the established phase diagram, standard Gibbs energy changes of reactions, which appear in the

TABLE 2
The Phases under Invariant Conditions

Sample Pr_2O_3/CoO	"Break" points ($-\log P_{O_2}$)		Phases present under invariant conditions
	1100°C	1150°C	
6/4	10.33	9.70	Co, CoO, Pr_2O_3
	5.86	5.77	CoO, Pr_2O_3, Pr_2CoO_4
	3.95	3.60	Pr_2O_3, Pr_2CoO_4, $Pr_4Co_3O_{10}$
	2.75	2.40	Pr_2O_3, $Pr_4Co_3O_{10}$, $PrCoO_3$
	1.30	0.94	Pr_2O_3, PrO_x (σ-phase), $PrCoO_3$
3/5	10.33	9.70	Co, CoO, Pr_2O_3
	5.86	5.77	CoO, Pr_2O_3, Pr_2CoO_4
	4.24	4.00	CoO, Pr_2CoO_4, $Pr_4Co_3O_{10}$
	3.50	3.27	CoO, $Pr_4Co_3O_{10}$, $PrCoO_3$
	2.75	2.20	$Pr_4Co_3O_{10}$, $PrCoO_3$, Pr_2O_3
	1.30	0.94	$PrCoO_3$, Pr_2O_3, PrO_x (σ-phase)
3/7	10.33	9.70	Co, CoO, Pr_2O_3
	5.86	5.77	CoO, Pr_2O_3, Pr_2CoO_4
	4.24	4.00	CoO, Pr_2CoO_4, $Pr_4Co_3O_{10}$
	3.50	3.27	CoO, $Pr_4Co_3O_{10}$, $PrCoO_3$

be used in the calculation of activity of the components in the solid solutions using the Gibbs–Duhem equation (13). Here, N_O and $N_{component}$ are the mole fraction of oxygen and component (cf. Table 1) in the solid solutions, respectively. The a and b values, which were obtained from thermogravimetric results, for Pr_2CoO_4, $Pr_4Co_3O_{10}$, and $PrCoO_3$ at 1100°C are 6.11×10^{-3} and 0.181, 0.0517 and 0.140, and 0.0442 and 0.0493, respectively, and those at 1150°C 0.0290 and 0.253, 0.0217 and 0.0592, and 0.0362 and 0.0250, respectively.

3. Pr_2O_3–Co–Co_2O_3 System at 1150°C

Seven samples with Pr_2O_3/CoO mole ratios were prepared for use in thermogravimetry. The phase diagram depicted based upon these thermogravimetric results and the identification of phase shows the same pattern as those at 1100 and 1200°C. The stability range of the oxygen partial pressure of solid solutions and activities of the components in the solid solutions are also tabulated in Table 1.
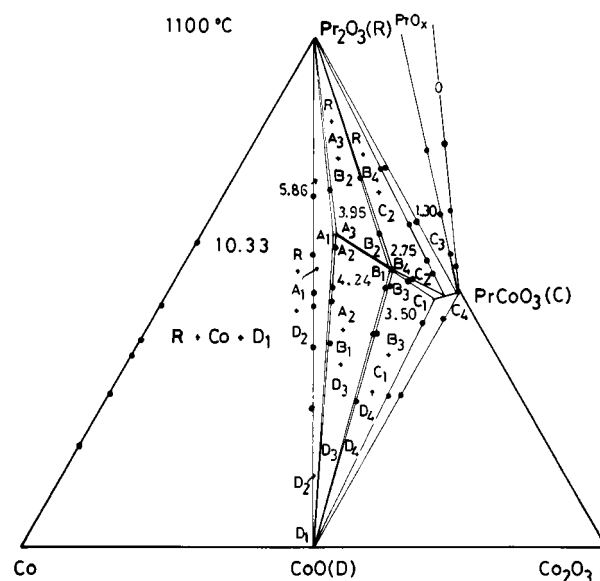
TABLE 3
The Standard Gibbs Energy Change of Reactions

Reaction	Temperature (°C)	$-\log P_{O_2}$ (atm)	$-\Delta G°^a$ (kJmol^{-1})
[1] $Pr_4Co_3O_{10} + 1/4\ O_2$	1100	2.75	19.7
$= 1/2\ Pr_2O_3 + 3PrCoO_3$	1150	2.20	18.0
	1200	2.05	15.8
[2] $Pr_4Co_3O_{10} + CoO + 1/2\ O_2$	1100	3.50	45.4
$= 4PrCoO_3$	1150	3.27	44.4
	1200	3.05	41.7
[3] $3Pr_2CoO_4 + 1/2O_2$	1100	3.95	63.6
$= Pr_4Co_3O_{10} + Pr_2O_3$	1150	3.65	59.9
	1200	3.10	58.4
[4] $2Pr_2CoO_4 + CoO + 1/2O_2$	1100	4.24	63.6
$= Pr_4Co_3O_{10}$	1150	4.00	60.2
	1200	3.60	57.3
[5] $Pr_2O_3 + CoO + 0.004O_2$	1100	5.86	6.2
$= Pr_2CoO_{4.08}$	1150	5.77	6.3
	1200	5.73	6.1
[6] $Co + 1/2O_2 = CoO$	1100	10.33	135.8
	1150	9.70	132.2
	1200	9.30	131.1

^{a} ±1.0 kJmol^{-1}.

phase diagram and are shown in Table 3, are determined with an equation, $\Delta G° = -RT \ln K$. Here, R is the gas constant, T is the absolute temperature, and K is the equilibrium constant of the reaction. Activities of the components in the solid solutions, which are necessary to calculate K values, are tabulated in Table 1. The standard state of the component in the solid solutions can be arbitrarily chosen for each solid solution and it is indicated as $\log a_i = 0$ in Table 1. $\Delta G°$ values for the reactions are tabulated in Table 3 together with those of 1200°C (1). Assuming that activities of the components in the solid solutions are unity, $\Delta G°$ values for reactions [3] and [4], for example, in Table 3 are -51.9 and -55.8 kJmol^{-1} at 1100°C, and -49.7 and -54.5 kJmol^{-1} at 1150°C, respectively. The differences in both values are significant and the activity of the component in the solid solutions must be used to determine K values.

REFERENCES

1. K. Kitayama, *J. Solid State Chem.* **77,** 366 (1988).
2. R. Flamand and R. Berjoan, *High Temp. High Pressures* **15,** 693 (1983).
3. D. Demazeau, M. Pouchard, and P. Hagenmuller, *J. Solid State Chem.* **9,** 202 (1974).
4. M. V. Kniga, I. I. Vygouskii, and E. E. Klementovich, *Zh. Neorg. Khim.* **24,** 1171 (1979).
5. V. A. Cherepanov, A. N. Pertov, and L. Yu. Grimova, *Zh. Fiz. Khim.* **59,** 2131 (1985).
6. K. Kitayama, *J. Solid State Chem.* **73,** 381 (1988).
7. K. Kitayama and T. Katsura, *Bull. Chem. Soc. Jpn.* **58,** 948 (1985).
8. K. Kitayama, *J. Solid State Chem.* **137,** 255 (1998).
9. B. G. Hyde, B. J. M. Bevan, and L. Eyring, *Phil. Trans. Roy. Soc. A* **259,** 583 (1966).
10. R. P. Turcotte, J. M. Warmkessel, R. J. D. Tilley, and L. Eyring, *J. Solid State Chem.* **3,** 265 (1971).
11. S. Ramdas, K. C. Patil, and C. N. R. Rao, *J. Chem. Soc. A* **64** (1970).
12. T. Sugihara, thesis, Tokyo Institute of Technology, 1978.
13. K. Kitayama, K. Nojiri, T. Sugihara, and T. Katsura, *J. Solid State Chem.* **56,** 1 (1985).